Phase separation frustrated by the long-range Coulomb interaction. II. Applications

J. Lorenzana,[1,2] C. Castellani,[1] and C. Di Castro[1]
[1]*Dipartimento di Fisica, Università di Roma "La Sapienza" and Istituto Nazionale di Fisica della Materia, Unità di Roma I, Piazzale A. Moro 2, I-00185 Roma, Italy*
[2]*Consejo Nacional de Investigaciones Científicas y Tecnicas, Centro Atómico Bariloche, 8400 S. C. de Bariloche, Argentina*
(Received 29 May 2001; published 3 December 2001)

The theory of first-order density-driven phase transitions with frustration due to the long-range Coulomb (LRC) interaction developed in paper I of this series is applied to the following physical systems: (i) the low-density electron gas, (ii) electronic phase separation in the low-density three-dimensional t-J model, and (iii) in the manganites near the charge-ordered phase. We work in the approximation that the density within each phase is uniform and we assume that the system separates into spherical drops of one phase hosted by the other phase with the distance between drops and the drop radius much larger than the interparticle distance. For (i) we study a well-known apparent instability related to a negative compressibility at low densities. We show that this does not lead to macroscopic drop formation as one could expect naively and the system is stable from this point of view. For (ii) we find that the LRC interaction significantly modifies the phase diagram favoring uniform phases and mixed states of antiferromagnetic (AF) regions surrounded by metallic regions over AF regions surrounded by empty space. For (iii) we show that the dependence of local densities of the phases on the overall density found in paper I gives a nonmonotonous behavior of the Curie temperature on doping in agreement with experiments.

DOI: 10.1103/PhysRevB.64.235128 PACS number(s): 71.10.Hf, 64.75.+g, 71.10.Ca, 75.30.Vn

I. INTRODUCTION

In the last decades continuous progress in the characterization and preparation of complex compounds has produced a variety of systems with very rich phase diagrams when the concentration of some dopant is varied. Notable examples includes doped cuprates and manganites where one finds different phases as the electronic density is varied. Quite generally and in analogy with familiar first-order phase transitions, like the ice-liquid transition, it is natural to ask under what conditions one can find ranges of global electronic density with phase separation among the many electronic phases that one finds in these materials.[1,2]

This problem has arisen naturally for doped Mott insulators[3,4] and Fermi liquid instabilities[5] in the context of the cuprates and also in the related problem of doped magnetic semiconductors.[6]

It is by now settled that close to the Mott transition there is a natural tendency for the system to phase separate in insulator and metallic phases with different densities. This tendency is frustrated by the long-range interaction which tends to favor uniform phases. As a result the system can choose to phase separate in an inhomogeneous state with islands of one phase in the other phase keeping long-scale neutrality. The same phenomena can occur in a variety of situations and in particular in the doped magnetoresistant manganites phase separation at various scales is observed in different regions of the phase diagram.[7] Also there is evidence that the two-dimensional (2D) electron gas phase separates at low densities.[8]

In paper I of this series (hereafter referred as I) we have presented a theory of phase separation frustrated by the long-range Coulomb (LRC) interaction and in the presence of a surface energy cost. We showed that if the Coulomb and surface energy cost are not too strong, the phase-separated state survives but it is inhomogeneous. In a certain global density range drops of one phase (A) are formed and hosted by the other phase (B). The free energy per unit volume reads

$$f=(1-x)f_A(n_A)+xf_B(n_B)+e_m, \tag{1}$$

where x is the volume fraction. The first two terms are the bulk contribution of the A and B phases and the last term is the mixing energy

$$e_m=\left[\frac{\sigma^2e^2(n_B-n_A)^2}{\epsilon_0}\right]^{1/3}u(x), \tag{2}$$

where $u(x)$ is a geometric factor which in the case of drops is

$$u(x)=3^{5/3}\left(\frac{\pi}{10}\right)^{1/3}x(2-3x^{1/3}+x)^{1/3}. \tag{3}$$

The mixing energy includes the surface energy cost and the electrostatic cost.

In our computations we have assumed that the scales of the inhomogeneities are much larger than the interparticle distance. This study is complementary to others which have considered the opposite limit (frustrated phase separation at a scale comparable to the interparticle distance) to explain phenomena like the striped states in cuprates.[3,5]

We have considered spherical drops as done by Nagaev and collaborators in the context of doped magnetic semiconductors in general and of manganites in particular.[6,9] However, we obtain similar results in other geometries like a periodic array of layers and we believe that for any reasonable geometry similar behavior for thermodynamic quantities would be obtained.

To illustrate the generality of theses ideas in this paper we consider some relevant applications to open problems in condensed matter.

It is well known that the low-density electron gas has a negative compressibility.[10] We discuss the fundamental problem of the stability of the electron gas and of the Wigner crystal at low density against a bubble phase (Sec. II). The system is shown to be stable against this kind of phenomena, showing explicitly that a negative compressibility can be observed in this system because the LRC interactions make it stable. Interestingly negative compressibility has been measured in the 2D electron gas.[11]

To make a link with the problem of phase separation (PS) in doped Mott insulators we consider frustrated PS in the *t-J* model (Sec. III). This is one of the simplest models used in the context of high-temperature superconductors where frustrated phase separation is believed to play an important role. We illustrate the importance of the LRC forces in determining the phase diagram.

Finally we study the problem of phase separation in the manganites between a ferromagnetic metallic phase and a charge-ordered phase (Sec. IV). This problem illustrates nicely how the anomalous behavior of local densities found in I can be reflected in measurable quantities. We propose an explanation for the anomalous behavior of the Curie temperature close to a charge-ordered instability; i.e., the Curie temperature decreases as the charge-ordered instability is approached. We conclude with a summary of the main results (Sec. V).

II. STABILITY OF THE JELLIUM MODEL

Here we discuss the case of a system of electrons in a uniform rigid background usually called the ''jellium'' model. Although we find that drops do not form in this case, this first discussion is very useful to illustrate the range of applicability of the present ideas.

The problem is the following: It is well known that a low-density electron gas has a negative electronic compressibility.[10] Will this lead to drop formation?

To describe in an approximate way the electronic energy one can use the Wigner interpolation formula for the correlation energy. In this approximation the ground-state energy per particle at zero temperature is given by[10]

$$E_{el}/Ry = \frac{2.2099}{r_s^2} - \frac{0.9163}{r_s} - \frac{0.88}{r_s + 7.8}, \tag{4}$$

where the first term is the kinetic energy, the second term is the exchange energy, and the last term is the correlation energy. Here $r_s = [3/(4\pi n)]^{1/3}/a_0$ and a_0 is Bohr's radius.

The energy per unit volume is $f_{el}(n) = E_{el} n$. In Fig. 1 we plot f_{el} and E_{el} as a function of density. These curves can be interpreted in two different ways. If the background compressibility is given only by the electrostatic self-energy (already included), then the curves represent the total energy of the system, background plus electrons. We call this the compressible background case. Two different criteria give thermodynamic instability for the compressible background case.

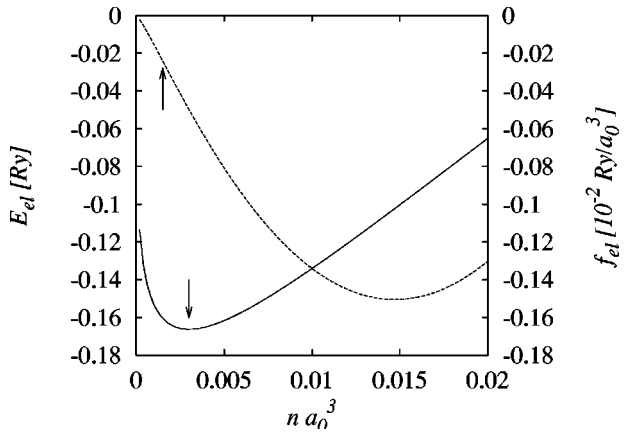

FIG. 1. Energy per particle (left axis, solid line) and per unit volume (right axis, dashed line) as a function of density obtained from the Wigner interpolation formula. The vertical arrows indicate the density at which the pressure is zero (lower one) and the density at which the jellium model contribution to the compressibility becomes zero (upper one). In the latter case the corresponding change of curvature is almost indistinguishable to the bare eye.

First for $na_0^3 < 0.0015$ (up arrow) the compressibility is negative. More importantly for $na_0^3 < 0.003 \equiv n_{el}^0$ (down arrow) the pressure is negative. The latter means that if the system is prepared with a density lower than n_{el}^0, then electrons and background will relax to a self-bound system with a lower volume and $n = n_{el}^0$ (from now on we shall measure densities in units of Bohr inverse volume a_0^3). We can consider this result as due to the usual Maxwell construction (MC) argument applied to phase separation between the electronic system+background and the vacuum. In fact it is easy to see that $n = n_{el}^0$ satisfies a MC in which the MC line intersects the origin. By applying an external pressure densities higher than n_{el}^0 become physically accessible. The numerical value of n_{el}^0 can change when more accurate forms of the correlation energy are considered, but the qualitative picture will remain the same.

The above interpretation is not useful in real situations where forces other than the electrostatic one can constrain the background to have a certain density. This leads to a second interpretation of the curves in Fig. 1. Since the background has additional nonelectrostatic contributions to the compressibility (for example, coming from core-core repulsion of the atoms), the plots of Fig. 1 are not anymore the total energy of the (neutral) system as a function of density.

A simple hypothesis to describe such a system is to assume in the model that the substrate is completely rigid. We call this the incompressible background case. The curves in Fig. 1 represent then the energy of many different realizations of this system, each with a different density. The energy includes the electrostatic cost to change the density of the background from one system to another but excludes the (infinite) nonelectrostatic energy cost to change the density of the background.

Now the total density is fixed at some value, the inverse compressibility of the whole system is infinite, and the above instability criteria do not apply anymore. This, however, does

not guarantee the stability of the system. One can imagine that the system may be unstable towards an inhomogeneous phase with electron-rich and electron-poor bubbles in the uniform fixed background.

We analyze below the case in which the electron-poor regions have zero electron density. In principle we can work as in I with a quadratic expansion of the free energy around the MC case; however, the free energy has now a simple form which can be dealt with analytically.

A. Electron drops in background

The compressible background case suggests that the system has the tendency to separate into electron-rich regions and regions of zero electron density. We will take the *A* and *B* phases of I to be the background with no electrons and the background with an undercompensated density of electrons, respectively. Consider first the case of low densities for the *B* phase. We can take for the bulk drop free energy the energy of a classical Wigner crystal, i.e., the leading $1/r_s$ term in Eq. (4) for large r_s. This microscopic Wigner crystal should not be confused with the mesoscopic Wigner crystal that the drops would form.

It is instructive to write the free energy in the following way:

$$f=\frac{6\pi e^2 n}{5}\left\{-n_{el}r_{el}^2+n_{el}R_d^2\left[2-3\left(\frac{n}{n_{el}}\right)^{1/3}+\frac{n}{n_{el}}\right]\right\}. \quad (5)$$

The volume fraction of the *B* phase *x* has been eliminated by using the constraint in the density given by $n=xn_{el}$ where $n_{el}\equiv 3/(4\pi r_{el}^3)\equiv n_B$ and $n_A=0$. The first term in the brackets comes from the classical Wigner crystal contribution (the leading term in $f_B\equiv f_{el}$ at low density) and the second term is the mixing energy contribution computed in I. The latter contains the electrostatic bubble contribution and the surface energy contribution. The radius is not a free parameter but $R_d\equiv R_d(n,n_{el},\sigma)$ is the drop radius that minimizes the free energy.

Notice that the drop of electrons is not neutral since the density of electrons is larger than the compensating background, i.e., within the drops we are dealing with a charged Wigner crystal of electrons in contrast with the usual neutral Wigner crystal of electrons. On the other hand, in the computation of the charging energies of the drops in I we have assumed for simplicity that the density is uniform inside the drop. In Appendix A of paper I we compute the correction to the electrostatic energy due to the nonuniform electronic density at the microscopic scale as it should be for a charged Wigner crystal and conclude that this only changes numerical factors, which are not important for the present analysis.

Since the drop radius has already been minimized, one is left with the density inside the drops (or equivalently with r_{el}) to be minimized. R_d depends on the density explicitly and indirectly on $\sigma(n_{el})$. If the last term in the curly brackets grows with n_{el} faster than $n_{el}r_{el}^2$, the minimum occurs at $n_{el}\to n$, i.e., $x=1$. This corresponds to the uniform case. If instead $n_{el}r_{el}^2$ grows faster, one finds a solution with $n_{el}\to\infty$; the term in the square brackets becomes a constant and clearly $r_{el}>R_d$. In this case the mesoscopic bubble model is clearly not adequate. In order for both terms to balance exactly one finds that the surface energy has to fulfill the relation $\sigma\sim e^2 n_{el}^{2/3}/r_{el}$. If one estimates the surface energy as a characteristic energy density ($n_{el}e^2/r_{el}$) times a characteristic length ($r_{el}\sim n_{el}^{-1/3}$), one can conclude on dimensional arguments that this surface energy is precisely the one of a Wigner crystal. Smaller surface energies give drops which are too small for the mesoscopic treatment and larger surface energies give no drops at all.

What about the other contributions to the bulk free energy in Eq. (4) which will become important as the density inside the drop becomes large? They only make the drop bulk term less negative, so an even smaller value of the drop radius is needed to stabilize the drop solution. From this point of view we can conclude that mesoscopic or macroscopic drops of electron gas are not possible.

The only dubious case could be close to $x=1$ ($n_{el}\to n$), since in this case the term in the square brackets can be very small. In principle this allows for large drops without paying too much mixing energy. However, in this region Eq. (5) is not strictly valid since the volume fraction is close to 1 and one has to revert the geometry as done below.

B. Drops of empty background (voids)

We consider the possibility of formation of drops of zero electronic density (voids) hosted by electron rich regions with density n_{el}.

We look again to the limit of the classical Wigner crystal. Now *x* will represent the fraction of empty electronic volume. The constraint in the density is given by $n=(1-x)n_{el}$ and the free energy reads

$$f=\frac{6\pi e^2}{5}\left\{-nn_{el}r_{el}^2+(n_{el}-n)n_{el}R_d^2\times\left[3-3\left(1-\frac{n}{n_{el}}\right)^{1/3}-\frac{n}{n_{el}}\right]\right\}. \quad (6)$$

We see that if $n_{el}\to n$, we can get $R_d\gg r_{el}$ with a small surface and electrostatic energy (the last term in the curly brackets). Using the density constraint to eliminate n_{el} in favor of *x* we find that for small *x* the free energy behaves as $n^2(-5r_0^2+6R_d^2)x$ with r_0 given by $n\equiv 3/(4\pi r_0^3)$. Clearly to have a minimum for small $x>0$ we need $R_d<r_0$ and the model does not apply. The full expression for the free energy taking into account the electron kinetic energy gives an even smaller sloop for the dependence of *f* on *x* so that an even smaller drop radius is obtained. We could still have drops with finite electronic densities in both the drop and the host phases. In this way one can reduce the mixing energy because it depends on the density difference n_B-n_A [Eq. (2)]. One could expect to find a solution close to the critical density for zero pressure n_{el}^0. We have searched for such a solution assuming $E_{el}\sim(n-n_{el}^0)^2$. It has higher energy than the uniform solution.

We can conclude that a 3D electron-jellium model is not unstable towards mesoscopic or macroscopic drop formation

and density regions where the compressibility of the electron gas is negative are physically accessible. Interestingly a negative compressibility is actually observed for the 2D electron gas.[11] Our result stems from the fact that both the energy gain coming from the MC and the energy cost have the same electrostatic origin. Of course we cannot discard instabilities that can occur at a microscopic scale.

III. FRUSTRATED PHASE SEPARATION IN THE 3D *T*-*J* MODEL

In the last few years it has become clear that many of the strongly correlated models used to describe high-temperature superconductors exhibits PS in some regions of parameter space.[1,2] Due to the strong anisotropy of these materials, usually 2D models are considered. In this section we apply the idea of a Wigner crystal of drops to PS in models of strongly correlated electrons on a lattice. We will consider, for simplicity and homogeneity with I and the other sections of the paper, isotropic 3D lattice models. We expect, however, that the results will remain qualitatively valid even for 2D models. Needless to say, the 3D models are interesting on their own right given the large class of strongly correlated materials where anisotropy is not important like doped C_{60}, magnetoresistant manganites, etc.

Usually in strongly correlated lattice models the Coulomb interaction is truncated to a distance of a few lattice sites and often only the on-site Hubbard U term is kept. The underlying assumption is that in a uniform ground state most of the interesting physics is governed by the short-range interactions and that the effect of the long-range interactions can be absorbed in the Madelung potential through a proper Hartree renormalization of the on-site energies. However, in a nonuniform ground state the long-range part of the interaction has an important role even at the Hartree level. A simple way to take this into account is to maintain the relevant short-range interactions (e.g., the Hubbard U), to evaluate the energy of the intrinsic A or B phase and to add the electrostatic and surface contributions of the drops to the total free energy. This means that we are still neglecting the Coulomb interaction at distances larger than the lattice constant a, as in the usual Hubbard model, but we keep the Coulomb repulsion for mesoscopic distances of the order of the inhomogeneity scale. In other words in the Fourier transform of the Coulomb potential, $4\pi e^2/q^2$, we maintain terms with wave vector q close to $q=0$ that do not cancel with the background and hence give a large contribution to the energy.

As an example of the relevance of this approach for strongly correlated systems we focus on the t-J model, one of the more often used models in the cuprates. The Hamiltonian is given by

$$H=-t\sum_{\langle ij\rangle,s} c^{\dagger}_{i,s}c_{j,s}+J\sum_{\langle ij\rangle}\left(\mathbf{S}_i.\mathbf{S}_j-\frac{1}{4}n_in_j\right),$$

where $c^{\dagger}_{i,s}$ creates an electron of spin s on the site i. Here n_i and $\mathbf{S}_i$ are the electron number and spin operators, respectively. Double occupation is not allowed and summations are extended to the nearest neighbor of a 3D cubic lattice. The large-J/t limit has been studied in detail in two[4,12,13] and more dimensions based on a large-d expansion.[14] We study the limiting case of a small number of electrons (hole doping close to 1). This is not particularly relevant for the cuprates but illustrates the issue of frustrated PS in a strongly correlated system.

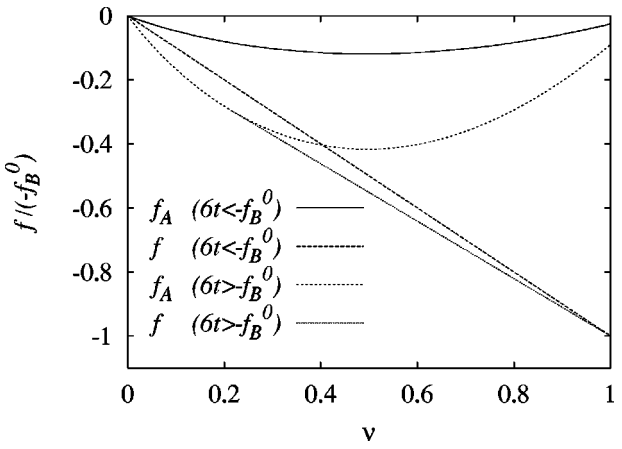

FIG. 2. Free energy normalized to the incompressible phase free energy without LRC and (from top to bottom close to the origin) the metal with $6t=0.6|f_B^0|$, PS between the AF and vacuum (AF+V), the metal with $6t=2.1|f_B^0|$, and MC phase separation between the AF and the metal (AF+M) ($n_B^0\equiv a\equiv 1$).

A. Maxwell construction analysis

We start by reviewing the usual MC arguments[4,14] in the absence of LRC adapted to the 3D case. The antiferromagnetic (AF) phase at half filling, hereafter the B phase, can be model by an incompressible phase with one electron per site. The density is given by $n_B=n_B^0=1/a^3$. Our densities refer to real electrons, not to holes. The energy is

$$f_B=f_B^0=-3bJn_B^0, \tag{7}$$

where bJ is the magnetic energy per bond. From estimates of the ground-state energy in the 3D Heisenberg model[14] one finds $b=0.550$.

Two different situations are found for the PS. For very large J/t one finds PS between the AF phase and the electron vacuum (AF+V). In this case we call the vacuum the A phase with $f_A=0$. Reducing J/t one finds PS between the AF phase and a dilute metal of electrons (AF+M). In this case we call the metal the A phase with energy

$$f_A(n_A)=-6tn_A+\frac{3^{5/3}}{5}\pi^{4/3}a^2n_A^{5/3}t. \tag{8}$$

Here t is the hopping matrix element and we have used the effective mass approximation in the dispersion relation of the low-density limit of the t-J model.[4,14]

In Fig. 2 we show the free energies in the absence of LRC and different values of $t/(-f_B^0)$. The total free energy is given by Eq. (1) with $e_m=0$. Since densities are assumed to be low, we can neglect the short-range interaction between

the electrons. We define the number of electrons per unit cell $\nu \equiv n/n_B^0$. In addition we set $a \equiv 1$ and restore it when convenient for clarity.

For very large J/t the AF+V solution is the lowest in energy. Indeed in Fig. 2 the upper curve corresponding to the uniform metallic energy does not intersect the AF+V line, $f = \nu f_B^0$, corresponding to the MC between the $\nu = 0$ and $\nu = 1$ points. Decreasing the value of J/t when the chemical potential of the metal fulfills $\mu_A(0)(=-6t) < f_B^0$, i.e., $t > bJ/2$, the metallic free energy intersects the AF+V free energy at some finite density and the lowest-energy state is achieved by doing the MC between the antiferromagnet and the metal. In this case as shown in Fig. 2, one finds a pure metallic phase at small density and MC phase separation between the AF and the metal for larger density. In Fig. 8, below, we show the phase diagram deduced from this analysis. The dilute metal can be unstable towards a gas of bound particles.[4,14] Here we do not consider this effect for simplicity.

In the next two subsections we analyze the effect of the LRC interaction on the AF+V PS and the AF+M PS. Since the electronic free energy has a simple form, we solve the equations exactly rather than making a linearization as in I.

B. Drops of an incompressible phase in vacuum (AF+V)

As shown above, in the absence of the LRC interaction, this case is realized in the large-J/t limit. Now we generalize the above discussion with the inclusion of LRC and surface energy effects. The A phase is the electron vacuum (V) ($n_A = 0$ and $f_A = 0$) and the B phase is the AF with one electron per site, $n_B = n_B^0 = 1/a^3$, and energy given by Eq. (7). The total free energy is given by Eq. (1) with the above replacements. An expansion of the densities around the MC solution (Sec. III of paper I) gives a trivial result since $\lambda = 0$ (notice that $k_m = 0$) and the densities are fixed at the MC values [Eq. (29) of paper I]. However, this is a peculiar limit. In fact as we will show below the total free energy does not coincide with the MC free energy because of the mixing energy. Since the densities are fixed, only the radius has to be determined which is given by Eq. (8) of paper I.

The surface energy of the AF is given by the energy cost to cut a bond divided by the associated surface $\sigma = bJ/a^2$ and the volume fraction is determined by the constraint $x = n/n_B^0 = \nu$. Inserting this into Eq. (8) of paper I we obtain

$$R_d = \left[\frac{15}{4\pi} \frac{bJ\epsilon_0}{(2 - 3\nu^{1/3} + \nu)e^2/a} \right]^{1/3} a. \tag{9}$$

As long as the dielectric constant is sufficiently large the radius is much larger than the lattice spacing and our approximations are valid.

By writing the free energy in dimensionless variables we can define a coupling constant that will determine the transition form the AF+V solution and the AF+M solution in the presence of LRC. It is given by

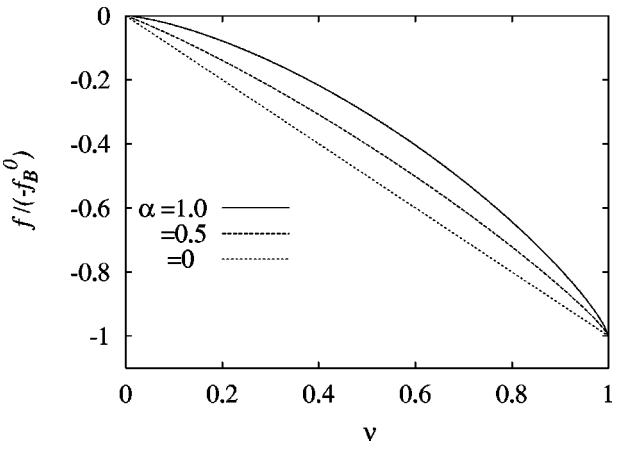

FIG. 3. $f/(-f_B^0)$ for a phase of drops of an incompressible phase in vacuum for $\alpha = 0,0.5,1,2$ (from bottom to top) vs ν.

$$\alpha = \frac{3}{-f_B^0} \left[\frac{9\pi e^2 \sigma^2 (n_B^0)^2}{5\epsilon_0} \right]^{1/3}. \tag{10}$$

Inserting the parameters for AF drops in Eq. (10) we find

$$\alpha^3 = \frac{9\pi}{5} \frac{e^2/a}{bJ\epsilon_0}, \tag{11}$$

i.e., the ratio of a Coulomb energy to a magnetic energy.

Imposing that $R_d > a$ for $\nu = 0$ one finds $\alpha < 3/2$, so we will concentrate on this range of coupling.

From Eqs. (1) and (3) we obtain the free energy as a function of density:

$$f(\nu) = \left[-\nu + \left(\frac{5}{243\pi} \right)^{1/3} \alpha u(\nu) \right] (-f_B^0). \tag{12}$$

The first term in the square brackets is the bulk contribution and the second term is the mixing energy contribution. This is plotted in Fig. 3 for different values of the coupling α. As in the above the results are only rigorously valid for small x ($= \nu$).

The effect of the mixing energy is to bend upwards the AF+V free energy (see Fig. 3) so that the metallic phase can become stable with a lower value of t with respect to the case with no LRC force (compare with Fig. 2). One can show that for $\alpha > 1$ the AF+V solution is never stable and one has either a uniform metal of an AF+M solution depending on doping. For $\alpha < 1$ the drops can coexist with a metal or not depending on the value of t/J. We will analyze the competition with the AF+M solution in the next section.

C. Drops of an incompressible phase in a metallic host (AF+M)

Reducing J/t at some point the solution of the previous section (AF+V) will not be stable any more. This has already been shown in the absence of LRC interaction ($\alpha = 0$). We consider now the A phase to be the metal.

The surface energy will have now density-dependent contributions coming from the metal. However, since we are in

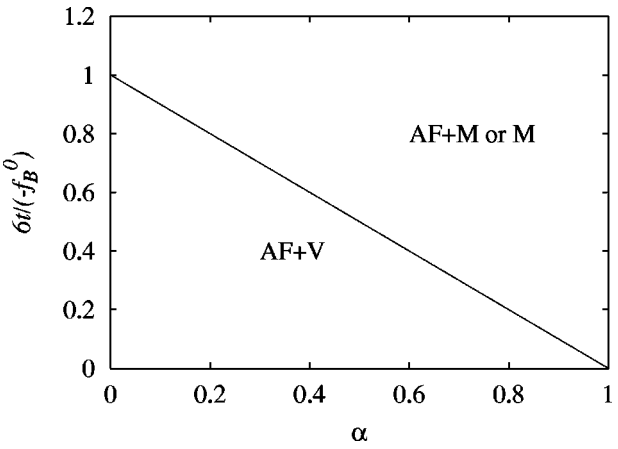

FIG. 4. Locus of stability of the AF drops in vacuum (AF $+V$) in the t-α plane. Above the line the more stable solution depends on the density.

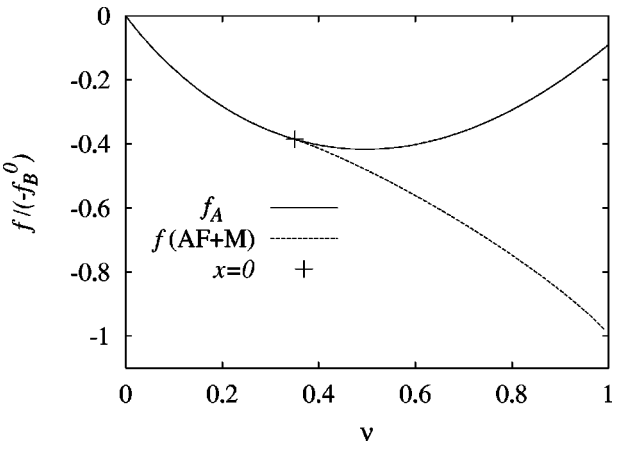

FIG. 5. Free energy normalized to the incompressible phase free energy with parameters $\alpha=0.5$ and $6t=2.1|f_B^0|$. We show the metallic free energy, the AF$+V$ free energy, and the AF$+M$ free energy. The cross indicates the value with $x=0$ of the AF$+M$ drop solution.

the low-density limit, the surface energy will be dominated by the magnetic surface energy described in the previous case and can be taken as constant. The AF$+V$ solution is then not anymore stable when $\mu_A(0)=-6t<\mu_{AF+V}(0)=(\alpha-1)(-f_B^0)$.

In Fig. 4 we show the locus of stability of the AF$+V$ solution in the t-α plane. Above the line the stable solution is either a uniform metal or drops of AF in the metal depending on the density. In Ref. 14 the ratio of J/t below which the AF$+V$ solution is not stable for $\alpha=0$ is called Y_c. In 2D they found $Y_c(0)=3.4367$ and $Y_c(0)\to 4$ for $d\to\infty$.[14] Using their estimate of the 3D AF energy we have $Y_c(0)=3.637$. Figure 4 shows that Y_c (proportional to the critical value of $-f_B^0/6t$) increases with α. Remarkably in the presence of LRC forces a smaller t is enough to stabilize metallic phase regions. In other words, we can have a situation in which without LRC forces all the electrons are in a self-bounded AF state and as the LRC forces are switched on some electrons ''evaporate'' to form a dilute gas around the AF drops.

To solve for the AF$+M$ drop solution the free energy now has to be minimized with respect to the radius and the density of the metal subject to the constraint $n=xn_B^0+(1-x)n_A$. We are implicitly assuming that the density is not low enough to form a Wigner crystal of electrons. One can check that for reasonable parameters and increasing α the radius of the drop becomes of the order of the lattice constant much before an electronic Wigner crystal can form.

Above the boundary line on Fig. 4 one finds either a uniform metal or AF$+M$ depending on the density. This can be seen in Fig. 5 where we plot the free energies for $6t=2.1|f_B^0|$ and $\alpha=0.5$. Above a certain density $n_{bif}=\nu_{bif}/a^3$ we have the coexistence of AF drops in the metallic host. The behavior close to n_{bif} is very similar to the behavior for parabolic free energies in the uniform density approximation (UDA) of paper I.

Here also there is a bifurcation of the solution, and increasing the density, the AF drops appear with a nonzero value of the volume fraction. However, with the present parameters the initial volume fraction is very small (see Fig. 6).

As the B density grows the n_A density decreases due to the effect discussed in paper I. The B density is kept constant at n_B^0 due to the incompressibility. In Fig. 7 we show this behavior. In real systems this effect can be detected through physical properties which depend on the local densities as is discussed below for the manganites.

In Fig. 8 we show the phase diagram in the absence of LRC force ($\alpha=0$) and for $\alpha=0.5$. We see that a portion of the phase diagram in which a uniform solution is unstable towards PS without LRC, for $\alpha>0$, becomes stable and the AF$+M$ solution extends its region with respect to the AF $+V$ solution due to the ''evaporation'' effect.

IV. APPLICATION TO THE MANGANITES

As a further application we consider the magnetoresistant manganites[7] like $La_{1-y}Ca_yMnO_3$. In the last years strong experimental evidence has accumulated indicating that inhomogeneous phase separation occurs in these materials in certain regions of parameter space.[15–20]

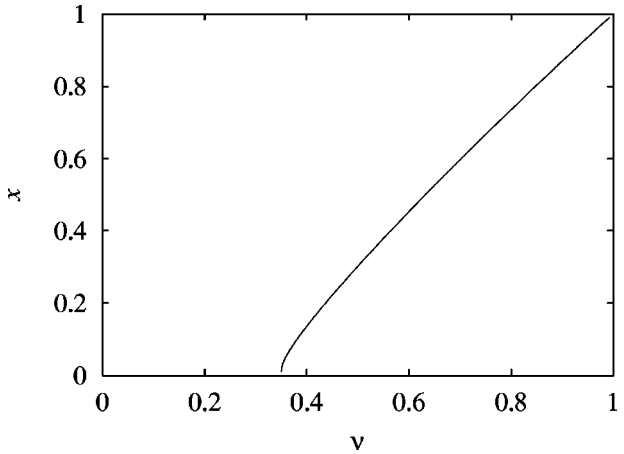

FIG. 6. Volume fraction vs ν for AF drops in a metallic host and parameters as in Fig. 5.

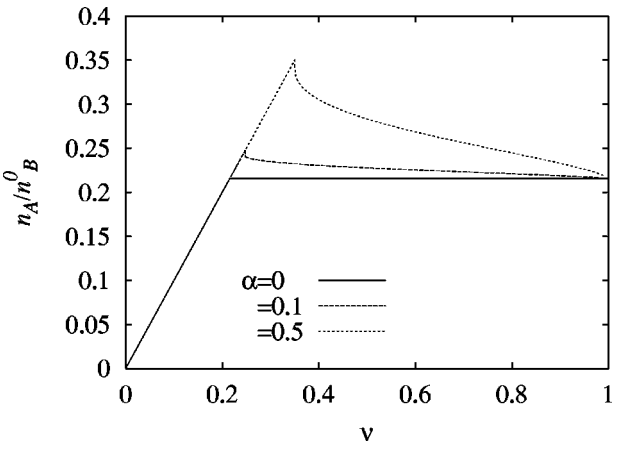

FIG. 7. Density in the metallic host vs total density ν for $6t=2.1|f_B^0|$ and different values of α.

At $y=0$ all Mn have formal valence $3+$. Each ion has three electrons in t_{2g} orbitals and one electron in an e_g orbital. The four electron spins are all parallel due to the strong Hund's rule coupling forming an $S=2$ spin. The spins of different Mn^{3+} ions form an antiferromagnetic phase due to the superexchange interaction and the system is an insulator. As the e_g band is doped, mobile holes tend to align the $S=3/2$ core (t_{2g}) spins in different ions because this maximizes the transfer integral and minimize the holes kinetic energy, leading to a ferromagnetic state. This is the so-called double-exchange (DE) mechanism.[21–23]

Experimentally one finds indeed the ferromagnetic state but close to $y=0.5$ a new charge-ordered (CO) insulating phase with a chessboard structure of Mn^{3+} and Mn^{4+} is stabilized. The CO phase is not predicted by conventional DE but does appear in more recent theories incorporating Mn-Mn Coulomb repulsion[24] or orbital degrees of freedom.[25]

Close to $y=0$ and $y=0.5$ the metallic ferromagnetic

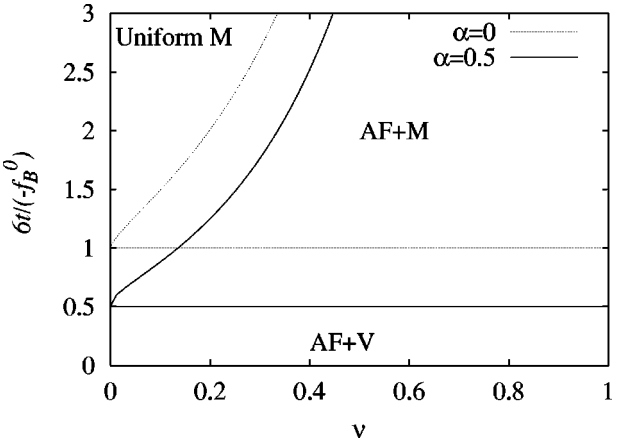

FIG. 8. Phase diagram for the large-J/t limit of the 3D t-J model without LRC ($\alpha=0$) and with a small LRC ($\alpha=0.5$). The high-density part has to be taken with care since the density of electrons can be large in the metal so that short-range interactions within the metallic phase cannot be neglected anymore, and also drops of AF lose sense.

(FM) phase competes with the corresponding insulating phase. The drop state due to the competition between the $y=0$ AF phase and the metallic phase taking into account the LRC interaction has been studied theoretically by Nagaev and collaborators.[6,9] Evidence for such a phase has recently been found in neutron scattering experiments.[18]

Here we will analyze the competition of the CO phase with the FM phase close to $y=0.5$ and show that a phase-separated state can explain the puzzling maximum of the Curie temperature $T_c(y)$ at $y\sim 0.35$.[26,27] On the contrary, conventional DE would predict that the Curie temperature is maximum at half doping ($y=0.5$) because for this filling the kinetic energy of the holes is maximized.

We will consider a mixed state in which the A phase is the ferromagnetic metal and the B phase is the charge order state at $y=0.5$ which corresponds to inverse specific volume $n_B^0=0.5/a^3$. In the following the densities refer to holes (i.e., the concentration of Mn^{4+} ions).

In the FM phase the core spins of the Mn ions are fully polarized and the mobile holes have the maximum bandwidth W. In order to model the FM in a simple fashion we follow Varma[28] and take a flat density of states with bandwidth W. The FM free energy at $T=0$ is then given by the cohesive energy of the holes in the fully polarized state:

$$f_A(n_A)=\frac{Wa^3}{2}(n_A-n_B^0)^2. \tag{13}$$

We have chosen to measure the single-particle energies from the center of the band and we have dropped a constant which can be absorbed in the free energy constant of the B phase f_B^0. At finite temperatures one has to consider the entropy contribution to the free energy. However, for a given temperature one can expand the full A free energy around the n_B^0 density and an expression like Eq. (13) is still valid with an effective temperature dependent W.

The CO state can be modeled as a doped incompressible phase around the inverse specific volume n_B^0. The free energy at $T=0$ can be put as

$$f_B(n_B)=\frac{E_G}{2}|n_B-n_B^0|+e_0(n_B-n_B^0)+f_B^0. \tag{14}$$

f_B^0 measures the difference in free energy per hole between the CO state and the FM state at $y=0.5$ ($n=n_B^0$) and e_0 controls the difference in chemical potentials of the two phases. E_G is the gap in the charge-ordered state, i.e., the difference between the energies to create defects with one added hole and one removed hole without destroying the CO state. (It should be of the order of the activation energy in the transport properties of a pure CO state.) The dip in the free energy at $n=n_B^0$ will become rounded with temperature. For simplicity we will neglect this effect. For temperatures much smaller than the gap, this is a good approximation. Even if the temperature gets comparable to the gap, a small rounding of the CO free energy close to $n_B=n_B^0$ will not affect significantly the results close to the density at which drops first appear (n_{bif}).

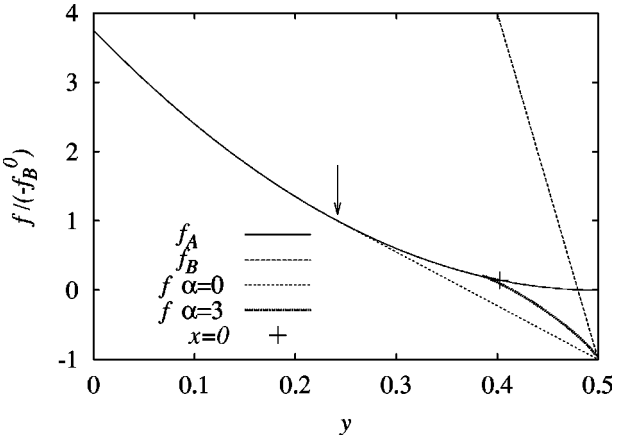

FIG. 9. Free energy normalized to the incompressible phase free energy at $y=0.5$ with a bandwidth $W=15|f_B^0|/n_B^0$. We show the FM free energy (f_A), the CO free energy with a large negative value of μ^-, and the FM+CO free energy for $\alpha=0$ (MC) and for $\alpha=3$. The cross indicates the value with $x=0$ of the FM+CO drop solution. The arrow indicates the same for the MC (y_0).

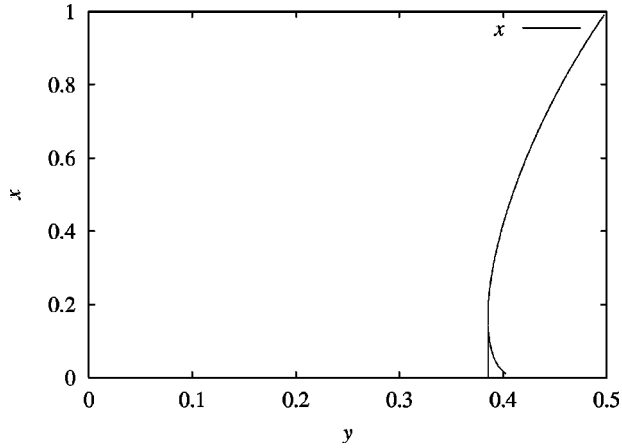

FIG. 10. Volume fraction vs y for CO drops in a FM host and parameters as in Fig. 9. The lower branch close to $y\sim0.4$ is unphysical.

The chemical potential of the CO state at $T=0$ is given by

$$\mu^+ = e_0 + E_g/2, \quad n_B > n_B^0, \tag{15}$$

$$\mu^- = e_0 - E_g/2, \quad n_B < n_B^0. \tag{16}$$

By construction the discontinuity at n_B^0 is equal to the gap as it should be. μ^- is the energy to create a Mn^{3+} defect in the CO state; i.e., it is the energy to remove a hole in the CO state. This single-particle energy is measured from the same reference energy as the one used for the A phase in Eq. (13). This fixes the value of e_0.

In Fig. 9 we have plotted f_A, f_B as a function of y. We constructed the free energies for the uniform phases phenomenologically by relying on the metallic and insulating character of each phase and on the fact that due to the different magnetic symmetries they cannot be joined with continuity but a level crossing should occur as a function of y. It is interesting to note that a recent microscopic model gives practically the same energy scheme as a function of doping.[25]

In Fig. 9 we report also the MC and the free energy for the drop solution for $\alpha=3$ and $W' \equiv W n_B^0/(-f_0^B)=15$ (thick line). The coupling constant α is defined in Eq. (10). W' measures the effective bandwidth in units of $(-f_0^B)$.

For the sake of simplicity we assume that the slope of f_B for $n_B<n_B^0$ (i.e., μ^-) is so large that f_B never crosses the drop solution. Under these simplifying conditions one of the phases involved in phase separation is always the defect-free CO state at $y=0.5$. In this situation E_g and e_0 do not enter into the problem and a precise description of $f_B(n_B)$ is not needed. For example we have neglected the kinetic energy of the defects which will give some curvature to $f_B(n_B)$ but will not change the present picture.

Alternatively to α we could use the coupling constant λ defined in Sec. III of paper I since the FM free energy is parabolic ($k_A^{-1}=k_m^{-1}=Wa^3$) and the CO free energy can be considered as the $k_B\to0$ limit of a parabola. The two coupling constants are related by

$$\lambda = \frac{2^{2/3}}{3}\frac{\alpha}{(W')^{1/3}}. \tag{17}$$

Specifically $\lambda=0.64$ for $\alpha=3$ and $W'=15$. Notice, however, that here (as in the previous section) we can introduce two dimensionless parameters. One is α (or alternatively λ) and the other is W'. The latter plays the same role as t/J in the previous section. In particular it fixes the MC densities as follows. In the absence of LRC interactions ($\alpha=0$) and for $W'<4$ the f_A parabola is too flat and PS between the FM and CO states is not possible. One gets PS between the CO state and vacuum (this is similar to the AF+V PS considered in Sec. III B). For $W'>4$ the Maxwell construction gives PS between FM and CO with the critical doping given by

$$y_0 = \frac{1}{2} - \frac{1}{\sqrt{W'}}. \tag{18}$$

In Fig. 9 the value of y_0 is indicated by an arrow.

In the presence of LRC interactions the range of coexistence contracts with respect to the Maxwell construction case. The transition from the FM to the drop solution is quite abrupt at $y_{bif}=0.38$ (for $\alpha=3$) with a substantial jump of the volume fraction from zero to a finite value $x_{bif}=0.17$ (see Fig. 10).

In Fig. 11 we show the local density inside the metallic region. For $y<y_{bif}$ the stable phase is uniform FM and the total density coincides with the nominal density $n=y/a^3$. For $y>y_{bif}$ the drop solution is stable and the density in the metallic region decreases with increasing nominal density. As discussed in paper I, in deriving this effect it is important that the density dependence of the surface energy can be neglected. The strongest dependence of the surface energy is expected to arise from the kinetic energy of the metal. However, this dependence is important close to $y\sim1$ and $y\sim0$ and can be safely neglected close to $y\sim0.5$.

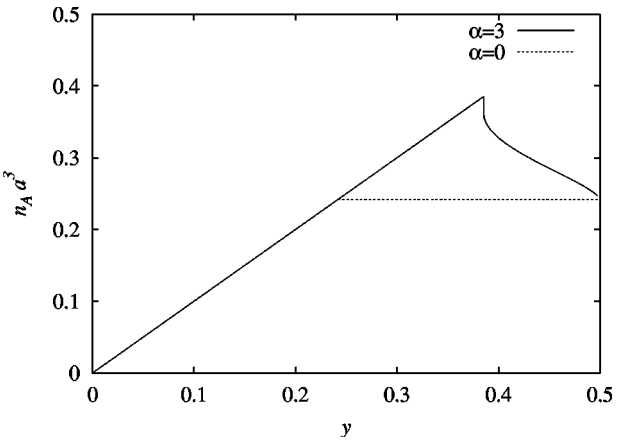

FIG. 11. Density in the metallic host vs doping y for parameters as in Fig. 9.

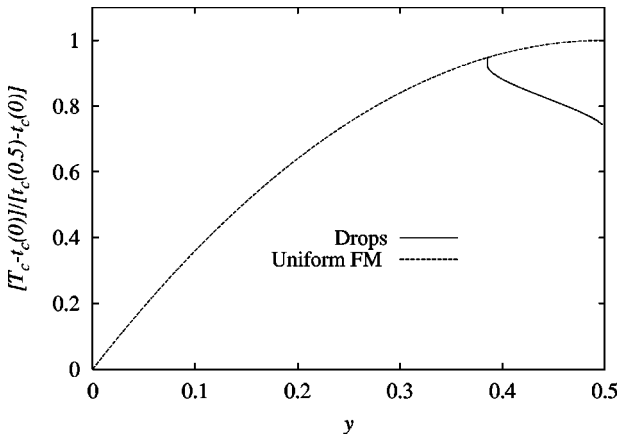

FIG. 12. T_c of the FM host minus $t_c(0)$ normalized to $t_c(0.5)-t_c(0)$ as a function of doping y. Parameters are as in Fig. 9. We show T_c in the uniform solution and in the drop solution.

The decrease of the local density with the increase of the global density can explain the nonmonotonous dependence of the Curie temperature T_c on y. Since the ferromagnetic interaction between the core Mn spins is mediated by the conduction electrons through the double-exchange mechanism, one expects the Curie temperature to be a monotonous increasing function of the local metallic density $n_A(<n_B^0)$ of the FM phase. We associate the region in which the Curie temperature increases with doping, i.e., the ''normal'' region (roughly $0.1<y<0.33$ for $La_{1-y}Ca_yMnO_3$), with a uniform FM phase and the ''anomalous'' regions in which the Curie temperature decreases with doping with a drop state. In the latter state n_A decreases with doping and this gives the anomalous behavior of T_c as a function of doping.

To be more specific we assume the following simple form for the dependence of the Curie temperature on the local FM density:

$$\frac{t_c(a^3n_A)-t_c(0)}{t_c(0.5)-t_c(0)}=4(1-a^3n_A)*a^3n_A\,. \tag{19}$$

We are using a lowercase t for the local Curie temperature of the FM phase to distinguish it from the true Curie temperature of the system which is a function of the overall doping, $T_c(y)$. A similar form to Eq. (19) with $t_c(0)=0$ was derived by Varma for a uniform FM phase.[28] More sophisticated treatments also give a form roughly parabolic with $t_c(0)>0$.[29]

For a uniform FM phase $y=n_Aa^3$, $T_c(y)=t_c(y)$. This fits correctly the experimental data in the normal region. We can use this fit to fix the parameters in Eq. (19). For $La_{1-y}Ca_yMnO_3$ one obtains $t_c(0)\sim 80$ K and $t_c(0.5)\sim 300$ K. Close to $y=0.5$ we have the anomalous behavior and the measured T_c differs considerably from $t_c(0.5)$, the Curie temperature of a hypothetically uniform phase. For example, experimentally $T_c(0.5)\sim 225$ K.

From the known $n_A(y)$ (Fig. 11) and Eq. (19) we compute $T_c(y)\equiv t_c[a^3n_A(y)]$. This curve (which is quite similar to the experimental one) is shown in Fig. 12. Indeed we see that the drop solution combined with the uniform solution for $y<y_{bif}$ gives a nonmonotonous behavior of $T_c(y)$. In evaluating the theoretical curve to be compared with the experimental data we fix the values of α and W' in the following way. We associate the experimental maximum in T_c with the bifurcation point, i.e., the doping at which the uniform solution switches to the drop solution. This gives us an experimental value of the bifurcation doping, $y_{bif}\sim 0.38$. From the experimental data we also obtain the depression of the Curie temperature $[T_c(0.5)-t_c(0)]/[t_c(0.5)-t_c(0)]\sim 0.66$. With these two dimensionless numbers we obtain the dimensionless parameters of our theory and find $\alpha=3$ and $W'=15$, i.e., the values that we have been using in the present section. A rough microscopic estimate of these parameters is given in the Appendix to show that indeed the above values are reasonable for the manganites.

A similar behavior as the one discussed here for $y\sim 0.5$ is observed close to $y\sim 0$. We speculate that this is due to the same general phenomena involving inhomogeneous phase separation between the insulator at $y=0$ and the ferromagnetic metal.

V. CONCLUSIONS

In this work we have applied the ideas developed in I to three different physical systems. First we analyzed well-known apparent instabilities in the low-density limit of the jellium model. The usual instability criteria like a negative compressibility are formulated for a neutral system and should be taken with care in a charged system with a compensating background. In a charged system an instability of the kind implied by a MC analysis is a necessary but not sufficient condition for mesoscopic phase separation. In fact we have seen that for the Wigner crystal of electrons the Coulomb strength and the surface energy balance in such a way that large drops are not possible. This is basically due to the fact that the energy gain from the MC and the energy cost due to the LRC interaction and surface energy have all the same electrostatic origin. This prevents the mixing energy from being small compared to the MC energy as required in I to have mesoscopic PS. We mention that in the 2D electron gas (not considered here) there is evidence for both a density

region of negative compressibilities and at lower densities a phase separation.[8,11] For the latter, however, the effect of disorder not considered by us may be crucial.

The study of the *t-J* model illustrates the importance of the mixing energy in determining the phase diagram. The LRC interaction tends to stabilize the nonseparated uniform phases in the presence of a rigid background. Apart from this intuitive effect the LRC interaction can also favor one mixed state over another. In fact we showed that the LRC interaction can transform the clusters of AF electrons in vacuum into clusters of AF electrons in equilibrium with its vapor (a dilute electron gas), a phenomenon which we referred to as ''evaporation.''

In paper I of this series we showed that the local densities of the two phases tend to have an anomalous behavior in the mixed state. Both of them tend to decrease when the global density increases. This nonlinear effect can affect the properties of the system which are sensitive to the local density, as we have illustrated for the Curie temperature in the manganites. We have thus provided an explanation to anomalies that occur in the phase diagram, i.e. a decreasing Curie temperature when the CO state is approached by varying the doping.

APPENDIX MICROSCOPIC ESTIMATE OF PARAMETERS IN THE MANGANITES

In Sec. IV we find that the parameters $\lambda=0.64$ and $W'=15$ give a curve $T_c(y)$ similar to the experimental one. To decide if these parameters are reasonable one needs a microscopic computation.

To evaluate W' which appears in Eq. (18) we refer to a recent zero-temperature microscopic computation which takes into account double exchange and orbital ordering.[25] Their Fig. 2 showing the free energy (without LRC) is quite similar to our $\alpha=0$ curves in Fig. 9. From there we take $y_0\sim 0.24$ which determines $W'\sim 15$ [Eq. (18)] in agreement with the value we used to fit T_c. λ is more difficult to obtain because it requires a microscopic computation of surface energies and screening effects. We parametrize the surface energy by a dimensionless quantity γ defined by $\sigma\equiv\gamma W/a^2$. Putting $\delta_0=(0.5-y_0)/a^3$ and $k_A^{-1}=k_m^{-1}=Wa^3$ in Eq. (25) of paper I we get

$$\lambda=2\left(\frac{9\pi}{5}\right)^{1/3}\frac{\gamma^{2/3}}{(0.5-y_0)^{4/3}}\left(\frac{e^2}{\epsilon_0 aW}\right)^{1/3}. \tag{A1}$$

For the bandwidth we can take an estimate based on Mattheiss's local density approximation (see Ref. 28), $W=2.5$ eV. For a cubic array of Mn with a Mn-Mn distance of 4 Å we get $e^2/a=3.4$ eV for the bare Coulomb strength. Inserting the numerical values in the above equation we have

$$\lambda\sim 21\left(\frac{\gamma^2}{\epsilon_0}\right)^{1/3}.$$

One obtains $\lambda\sim 0.64$, the value we have used in Sec. IV, by taking $\epsilon_0\sim 100$ and $\gamma\sim 0.05$. These are reasonable parameters considering that ϵ_0 should be understood as a static dielectric constant taking into account conventional dielectric screening plus Thomas-Fermi screening effects (Sec. IV of paper I) and γW should be a small fraction of the bandwidth.

We mention that since a real background is never perfectly rigid, a volume relaxation will also occur inside the drop phase. In general the positive background will contract in the electron-rich phase and expand in the electron-poor phase to reduce the mismatch between the ionic positive density and the electronic density. This is in agreement with the situation in $Pr_{0.7}Ca_{0.3}MnO_3$ where the electron-poor CO phase has a larger volume than the electron-rich FM phase.[17] Clearly this effect has to be included in the effective definition of ϵ_0.

The drop radius reads

$$R_d=\frac{32^{1/3}\gamma a}{\lambda[(\delta a^3)^2(0.5-y_0)^4(2-3x^{1/3}+x)]^{1/3}}. \tag{A2}$$

Using the above parameters we can estimate the radius at the onset ($x_{bif}=0.17$) to be of the order of

$$R_d\sim 10a.$$

Correspondingly the cell radius is $R_c=R_d/x^{1/3}\sim 18a$. We see that these scales are much larger than the lattice constant and our approximations apply.

[1] *Phase Separation in Cuprate Superconductors*, edited by K. A. Muller and G. Benedek (World Scientific, Singapore, 1992).

[2] *Phase Separation in Cuprate Superconductors*, edited by E. Sigmund and K. A. Muller (Springer-Verlag, Berlin, 1993).

[3] U. Löw, V.J. Emery, K. Fabricius, and S.A. Kivelson, Phys. Rev. Lett. **72**, 1918 (1994).

[4] V.J. Emery, S.A. Kivelson, and H.Q. Lin, Phys. Rev. Lett. **64**, 475 (1990).

[5] C. Castellani, C. Di Castro, and M. Grilli, Phys. Rev. Lett. **75**, 4650 (1995).

[6] E. Nagaev, *Physics of Magnetic Semiconductors* (MIR, Moscow, 1983).

[7] A. Moreo, S. Yunoki, and E. Dagotto, Science **283**, 2034 (1999).

[8] S. Ilani, A. Yacoby, D. Mahalu, and H.P. Shtrikman, Phys. Rev. Lett. **84**, 3133 (2000).

[9] E. Nagaev, A.I. Podel'shchikov, and V.E. Zil'bewarg, J. Phys.: Condens. Matter **10**, 9823 (1998).

[10] G. D. Mahan, *Many Particle Physics* (Plenum, New York, 1990).

[11] J.P. Eisenstein, L.N. Pfeiffer, and K.W. West, Phys. Rev. Lett. **68**, 674 (1992); S. Shapira, U. Sivan, P.M. Solomon, E. Buchstab, M. Tischler, and G. Ben Yoseph, *ibid.* **77**, 3181 (1996).

[12] M. Calandra, F. Becca, and S. Sorella, Phys. Rev. Lett. **81**, 5185 (1998).

[13] S.R. White and D.J. Scalapino, Phys. Rev. B **61**, 6320 (2000).

[14] E.W. Carlson, S.A. Kivelson, Z. Nussinov, and V.J. Emery, Phys. Rev. B **57**, 14 704 (1998).
[15] J.W. Lynn, R.W. Erwin, J.A. Borchers, Q. Huang, A. Santoro, J.L. Peng, and Z.Y. Li, Phys. Rev. Lett. **76**, 4046 (1996).
[16] J.M. De Teresa, M.R. Ibarra, P.A. Algarabel, C. Ritter, C. Marquina, J. Blasco, J. García, A. Del Moral, and Z. Arnold, Nature (London) **386**, 256 (1997).
[17] D.E. Cox, P.G. Radaelli, M. Marezio, and S.W. Cheong, Phys. Rev. B **57**, 3305 (1998).
[18] M. Hennion, F. Moussa, G. Biotteau, J. Rodriguez-Carvajal, L. Pinsard, and A. Revcolevschi, Phys. Rev. Lett. **81**, 1957 (1998).
[19] M. Uehara, S. Mori, C. Chen, and S.-W. Cheong, Nature (London) **399**, 560 (1999).
[20] G. Papavassiliou, M. Fardis, M. Belesi, T.G. Maris, G. Kallias, M. Pissas, D. Niarchos, C. Dimitropoulos, and J. Dolinsek, Phys. Rev. Lett. **84**, 761 (2000).
[21] C. Zener, Phys. Rev. **82**, 403 (1951).
[22] P.W. Anderson and H. Hasegawa, Phys. Rev. **100**, 675 (1955).
[23] P.G. de Gennes, Phys. Rev. **118**, 141 (1960).
[24] M.Y. Kagan, D.I. Khomskii, and M.V. Mostovoy, Eur. Phys. J. B **12**, 217 (1999).
[25] J. van den Brink, G. Khaliullin, and D. Khomskii, Phys. Rev. Lett. **83**, 5118 (1999).
[26] P. Schiffer, A.P. Ramirez, W. Bao, and S.-W. Cheong, Phys. Rev. Lett. **75**, 3336 (1995).
[27] K.H. Kim, M. Uehara, and S.-W. Cheong, cond-mat/0004467 (unpublished).
[28] C.M. Varma, Phys. Rev. B **54**, 7328 (1996).
[29] S. Okamoto, S. Ishihara, and S. Maekawa, Phys. Rev. B **61**, 451 (2000).